

## DEVELOPMENT OF THE SiC MUON BEAM MONITOR FOR THE COMET EXPERIMENT

Yoshinori Fukao\*, Yowichi Fujita, Tetsuichi Kishishita, Hajime Nishiguchi, Masayoshi Shoji,  
High Energy Accelerator Research Organization (KEK)

Kazutoshi Kojima, Ryouji Kosugi, Keiko Masumoto, Yasunori Tanaka,  
National Institute of Advanced Industrial Science and Technology (AIST)

### Abstract

A new detector to monitor a profile of a secondary muon beam for the COMET experiment is being developed. The COMET experiment searches for the muon-to-electron ( $\mu$ - $e$ ) conversion without emitting neutrinos. The discovery of the  $\mu$ - $e$  conversion is an evidence of the physics beyond the standard model of the particle physics. To achieve the goal of the experiment, it is important to suppress any fake signals. The new beam monitor is useful to assure a stability of the beam operation. The detector utilizes silicon carbide semiconductor expecting its high radiation tolerance because the high-intensity secondary beam of COMET can cause a significant radiation damage to the detector. We introduce the current status of the development of the muon beam monitor.

### INTRODUCTION

A construction of the COMET experiment is underway at J-PARC. The experiment aims to search for a process of the  $\mu$ - $e$  conversion. If it is discovered, it is a solid evidence of an existence of a new physics because the  $\mu$ - $e$  conversion is strongly prohibited in the standard model of the particle physics.

We are newly developing a detector to monitor a secondary muon beam. Due to a high radiation level at the detector location, we utilize a silicon carbide (SiC) semiconductor for a detection of the beam particles because the SiC semiconductor has higher radiation tolerance than a often-used silicon semiconductor. The development of the detector is ongoing in a cooperative framework of KEK Institute of Particle and Nuclear Studies and AIST Advanced Power Electronics Research Center.

### COMET EXPERIMENT

Figure 1 displays the COMET Phase-1 experimental setup [1]. The J-PARC proton beam is injected to a graphite Pion Production Target. The beam energy and intensity are 8 GeV and  $2.5 \times 10^{12} \text{ sec}^{-1}$ , respectively. The target is positioned in a 5-Tesla superconducting solenoidal magnet (Capture Solenoid) to capture as many secondary pions as possible. The pions are transported by a 3-Tesla superconducting curved solenoidal-magnet (Transport Solenoid). During the transportation, the pions are decayed to the muons. The muons are injected to an aluminum Muon Stopping Target and they form muonic atoms with the target material. A part

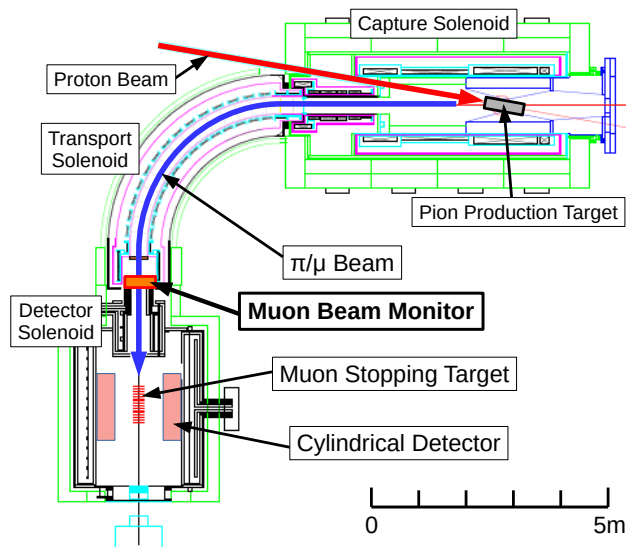


Figure 1: COMET Detector.

of the muons are captured by the nucleus and the remaining muons decay to electrons. In the standard model the decay electrons accompanied by two neutrinos have maximum energy of about 50 MeV, while in the  $\mu$ - $e$  conversion they hold about 105 MeV which is equivalent to the muon mass. To catch the signal of the  $\mu$ - $e$  conversion, the momentum of the electrons is measured by the COMET Cylindrical Detector (CyDet), whose main detector is a large cylindrical drift chamber surrounding the Muon Stopping Target. The proton beam has a bunch structure with interval of  $\sim 1.2 \mu\text{sec}$  or  $1.7 \mu\text{sec}$ . This feature is important because we have to avoid a beam-related prompt background in the decay electron measurements by selecting a time window between the proton beam bunches.

An intensity of the muon beam is estimated to be about  $10^{10} \text{ sec}^{-1}$ . The momentum of the muon beam is required to be about 45 MeV/c (9.2 MeV in kinetic energy) to stop them at the Muon Stopping Target. Any detectors to measure the secondary beam were not included at the original experimental setup because they can cause a loss of the useful muons and a production of background particles. However a control and an optimization of the muon beam is quite difficult without a beam monitor. We proposed the SiC muon beam monitor with thin material to minimize above demerits.

\* fukao@post.kek.jp

## MUON BEAM MONITOR WITH SiC SEMICONDUCTOR

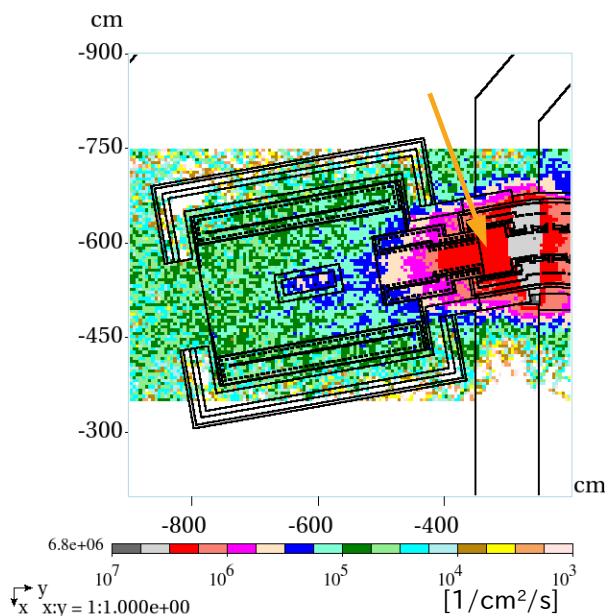


Figure 2: Simulated neutron fluence. The arrow indicates the position of the muon beam monitor.

One of the difficulties of the detector design comes from a middle-range intensity of the muon beam. Compared to a normal secondary beam, the COMET muon beam has higher intensity and a high radiation tolerance is required for the beam monitor. On the other hand, compared to the primary beam, its lower intensity requires higher signal gain for the detector. The radiation level was evaluated by the MARS simulation [2]. Figure 2 displays a neutron fluence around the position of the muon beam monitor. The 1-MeV equivalent neutron fluence at the monitor was  $1.6 \times 10^{13} \text{ cm}^{-2}$  at a proton-on-target of  $4.3 \times 10^{19}$ , which is an expected statistics during the COMET Phase-1 period. An ionizing damage was mainly caused by the beam particles to be 1.2 MGy, where about half of them is from the muons and the rest is from other charged particles such as electrons and positrons.

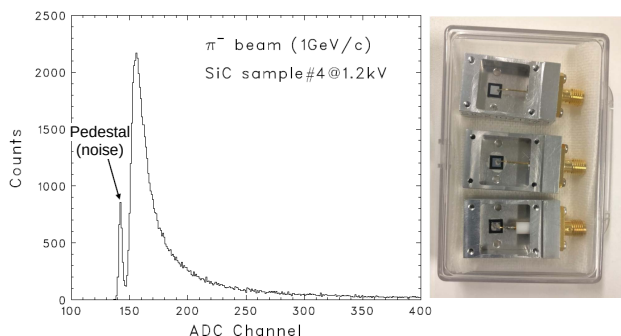


Figure 3: ADC distribution measured with J-PARC 1-GeV/c pion beam. A photo of the right hand side shows three prototypes of single channel.

To overcome the high radiation level, we utilize SiC semiconductor as a sensor of the detector. SiC has higher radiation tolerance than Si because it has a wide band gap of 3.26 eV and a displacement threshold energy of 22–35 eV. Our SiC semiconductor processed at AIST has a total thickness of  $\sim 350 \mu\text{m}$  and  $\sim 50\text{-}\mu\text{m}$  epitaxial layer [3]. Some single-channel prototype were manufactured and irradiated using J-PARC 1 GeV/c pion beam to evaluate the performance of the SiC semiconductor. Figure 3 displays ADC distribution and one can see clear MIP peak.<sup>1</sup>

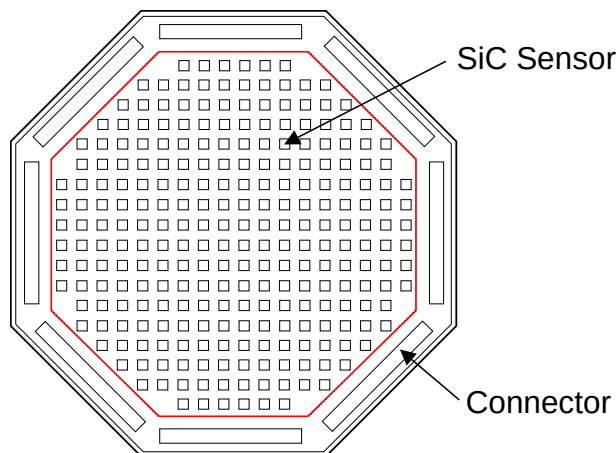


Figure 4: Schematic diagram of the muon beam monitor. Its width is about 220 mm.

Figure 4 is a schematic diagram of the muon beam monitor. Small squares indicate SiC sensor and have a size of  $5 \times 5 \text{ mm}^2$ . They will be mounted on the polyimide circuit board with a thickness of about  $200 \mu\text{m}$ . The circuit board will have two layers; one is for signal lines and the other is for the high-voltage. The signal wires will run between SiC sensors and will be connected to downstream front-end readout electronics via 8 connectors located at the edge of the detector. Because the circuit board is so thin that it needs mechanical support to self-stand, the edge region of the detector, which is outside of a red lines in Fig. 4, is thick to be 1.6 mm.

## SIGNAL ESTIMATION AND SIGNAL READOUT SCHEME

Time and position distribution of the secondary beam at the position of the muon beam monitor were evaluated using GEANT4 simulation. Figure 5 displays time distribution for each particle species. Most of the positively charged particles are discarded because they are not transported by the curved Transport Solenoid. Because many electrons and positrons hit the beam monitor at the prompt timing, the

<sup>1</sup> The measurements were performed using a commercial signal amplifier. Though the signal-to-noise (S/N) was good because the amplifier has long time constant of the order of micro-second, S/N will become worse at the actual use because a fast amplifier of less than 100 nsec will be required. However, due to the bunched beam, sufficient signal amplitude will be expected at the real measurements.

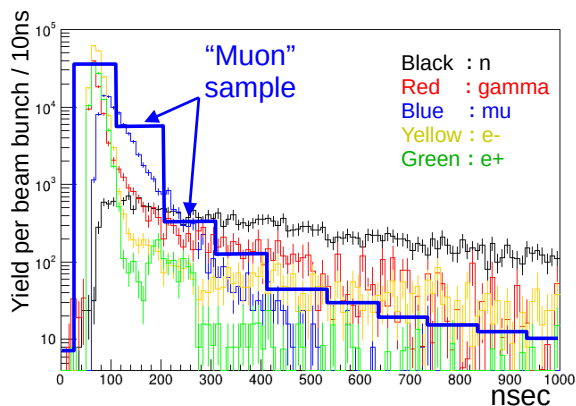


Figure 5: Hit time distribution of secondary particles. A wide blue line is a eye-guide of the sum of the charged particles with 100-nsec bin.

monitor needs to limit a detection time window to extract muons. Figure 6 displays horizontal position distribution with and without timing window of 100 to 300 nsec selected. The muon distribution can be extracted by selecting the time window.

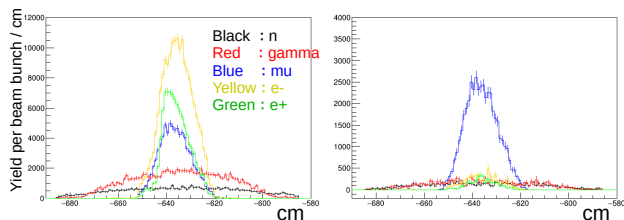


Figure 6: Horizontal hit position distribution of the secondary beam particles. The left and the right figures are the distribution without and with 200-nsec time window selected, respectively.

To realize applying the time window for the measurements, we plan to record the signal as a waveform with rough time resolution such as 100 nsec. The blue line in Fig. 5 shows the idea. Recorded data will have a shape like the blue line and the time window selection will be realized by selecting the second and the third bin from the peak bin. As well as the muon sample, we will be able to extract other background particles when we choose other bins. The ADC function described here will be implemented in ASIC (Application Specific Integrated Circuit) with high radiation tolerance. Because the front-end electronics must be installed near the detector where the radiation level will be high, any other ICs than ASIC can not be available there. The signal from the ASIC will be transported to another electronics for the signal driver that will be located outside of the Detector Solenoid in Fig. 1. The first prototype of the ASIC was produced and its evaluation is ongoing. Figure 7 is a photo of an evaluation board for the ASIC.

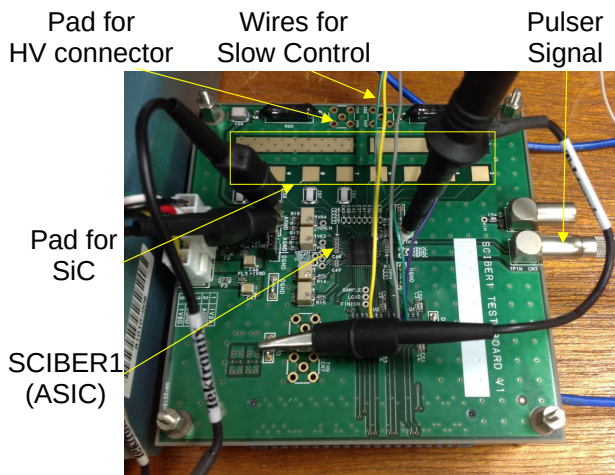


Figure 7: The evaluation board for the ASIC.

### SIGNAL LOSS AND BACKGROUND INCREASE

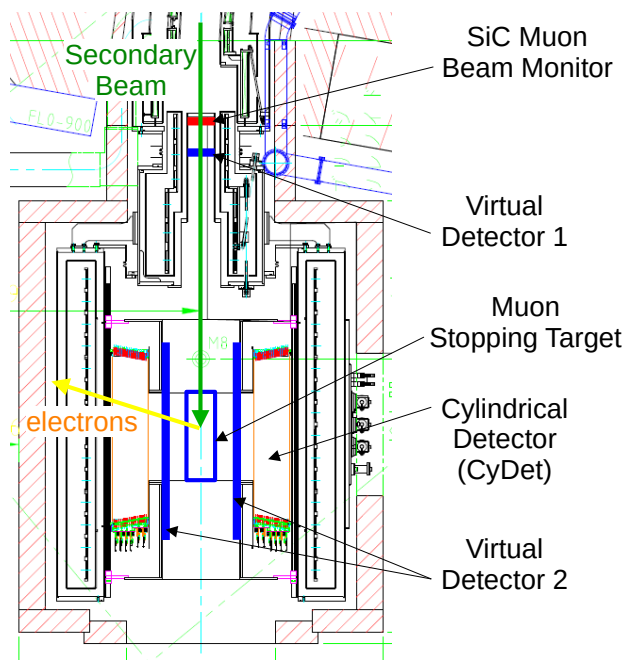


Figure 8: The setup of the GEANT4 simulation to evaluate the harmful effects by installing the beam monitor in the physics measurements.

The muons which is useful for the physics measurements will be reduced by installing the muon beam monitor because the low-momentum muons can be stopped at the detector. At the same time, an interaction of the beam particles and the muon beam monitor can produce background particles. We evaluated such harmful effects using GEANT4 simulation. Figure 8 displays a setup of the GEANT4 simulation. We assumed the beam monitor thickness as sum of 350  $\mu\text{m}$ -SiC, 175- $\mu\text{m}$  polyimide and 36- $\mu\text{m}$  copper. Two virtual detectors were located in the simulation and particles which penetrate

the virtual detectors were counted. In addition, the number of beam particles which stopped in the Muon Stopping Target was counted. Above counts with the SiC muon beam monitor installed ( $N_{w/\text{monitor}}$ ) and those without the monitor installed ( $N_{w/o\text{ monitor}}$ ) were recorded in the simulation. By comparing these, the signal loss and the background increase can be estimated.

Table 1: Simulated particle loss and background increase. Numbers in the table is a ratio of the particle count with the beam monitor to that without the beam monitor. Regarding the numbers for the Virtual Detector2, particles which hit the detector 500 nsec after the proton injection were required. This timing cut will be applied in the real measurements to avoid the prompt background related to the proton beam bunch. “-” means that no events remained with statistics of the simulation.

Particle	Virtual Detector1	Target Stop	Virtual Detector2 ( $t > 500$ nsec)
$e^-$	0.968	-	0.983
$e^+$	0.841	0.927	0.696
$\mu^-$	0.944	0.982	-
$\mu^+$	0.633	0.697	-
$\pi^-$	0.978	1.174	-
$\pi^+$	0.813	0.569	-
$p$	1.971	-	0.915
$n$	1.060	-	0.976
$\gamma$	1.236	-	0.981

The ratio of  $N_{w/\text{monitor}} / N_{w/o\text{ monitor}}$  are summarized in Table 1. At the downstream of the muon beam monitor (Virtual Detector1), protons, neutrons and gammas are increased because they are generated by muons captured by nuclei. On the other hand, other particles are reduced. The number of muons which are stopped at the Muon Stopping Target is reduced to be 98.2 %, which is a little larger than 94.4 %; the ratio at the Virtual Detector1, because higher-energy muons, which were originally not stopped at the target, stopped at

the target due to a loss of the energy at the beam monitor. The number of stopped negative pions is increased and they can produce background particles by pion-nuclei capture process. However, absolute yield of the negative pions is less than 1 % of the muons and the effect is not significant. In this simulation, any particles which hit CyDet (Virtual Detector2) is the background source because  $\mu$ - $e$  conversion process is not included. It turned out that the background would not increase by installing the muon beam monitor. The maximum ratio at the Virtual Detector2 was 98.3 %, which is very close to the loss of the stopped muons at the target. This means that there will be no significant degradation in terms of the signal-to-noise ratio.

## SUMMARY AND FUTURE PROSPECTS

We are developing the new muon beam monitor with SiC semiconductor sensors for the COMET experiment. The monitor can be realized owing to the high radiation tolerance of SiC. It is rather new to use SiC as a particle detector. There are several difficulties in the development other than the radiation tolerance. One of them is the mechanical feasibility because the detector with thin film-like circuit board must self-stand and the SiC sensors must be mounted on the board. We are now preparing a small prototype of the detector to establish a method of the detector fabrication.

We expect the first beam for the COMET experiment in JFY2022 where a commissioning of the proton beam acceleration and the muon transportation by the Transport Solenoid will be carried out. The physics measurement is expected to be performed in JFY2024.

## REFERENCES

- [1] The COMET collaboration, “COMET Phase-I technical design report”, Prog. Theor. Exp. Phys. 2020, 033C01.
- [2] N. V. Mokhov *et al.*, “The MARS Code System User’s Guide Version 15(2016)”, FERMILAB-FN-1058-APC.
- [3] T. Kishishita *et al.*, “SiC p+n Junction Diodes Toward Beam Monitor Applications”, IEEE Trans.Nucl.Sci. 68 (2021) 12, 2787-2793.